www.elsevier.com/locate/memsci

OPTIMIZED DISTILLATION COUPLED WITH STATE-OF-THE-ART MEMBRANES FOR PROPYLENE PURIFICATION

Raúl Zarca, Alfredo Ortiz, Daniel Gorri, Lorenz T. Biegler, Inmaculada Ortiz

PII: S0376-7388(18)30390-9
DOI: https://doi.org/10.1016/j.memsci.2018.04.016
Reference: MEMSCI16100

To appear in: *Journal of Membrane Science*

Received date: 8 February 2018
Revised date: 5 April 2018
Accepted date: 10 April 2018

Cite this article as: Raúl Zarca, Alfredo Ortiz, Daniel Gorri, Lorenz T. Biegler and Inmaculada Ortiz, OPTIMIZED DISTILLATION COUPLED WITH STATE-OF-THE-ART MEMBRANES FOR PROPYLENE PURIFICATION, *Journal of Membrane Science,* https://doi.org/10.1016/j.memsci.2018.04.016

OPTIMIZED DISTILLATION COUPLED WITH STATE-OF-THE-ART MEMBRANES FOR PROPYLENE PURIFICATION

Raúl Zarca[1], Alfredo Ortiz[1], Daniel Gorri[1], Lorenz T. Biegler[2], Inmaculada Ortiz[1*]

[1] Department of Chemical and Biomolecular Engineering. University of Cantabria, Av. Los Castros 46, 39005 Santander, Spain

[2] Department of Chemical Engineering, Carnegie-Mellon University, 5000 Forbes Avenue, Pittsburgh, Pennsylvania 15213-3890, United States

Corresponding author. ortizi@unican.es

Abstract

The growing production of polyolefins, mainly polyethylene and polypropylene, currently demands increasing outputs of polymer-grade light olefins. The most commonly adopted process for the separation of olefin/paraffin mixtures is performed by energy intensive high pressure or cryogenic distillation, which is considered the most expensive operation in the petrochemical industry. The use of membrane technology offers a compact and modular solution for capital and energy savings, thanks to process intensification. In this work, we move one step forward in the design of hybrid propane/propylene separation systems, using computer aided modeling tools to identify economically optimal combinations of distillation and state-of-the-art membranes. A model is proposed to optimize a hybrid configuration, whereby the membrane performs the bulk separation and the distillation column is intended for the final product polishing, accounting for membrane investment cost and process operating expenses. The decision variables are the membrane area and the column reflux ratio, and the

model is able to calculate the optimal feed trays. The upper-bound properties of selected membranes, which define their performance and reliability criteria, have been studied, benchmarking the economic evaluation against conventional distillation in order to assess the expedience of a hybrid system implementation.

Keywords: Optimization, propylene, propane, hybrid distillation, membrane, mathematical model, process intensification.

Nomenclature

A	membrane permeation area [m^2]
C_p	heat capacity at constant pressure [J mol^{-1} K^{-1}]
C_v	heat capacity at constant volume [J mol^{-1} K^{-1}]
d	differentiable distribution function
E	feed stream
e	feed stream DDF
ΔH_{vap}	enthalpy of vaporization [J mol^{-1}]
h	set of model algebraic equations
J	molar flux [mol m^{-2} s^{-1}]
L	hollow fiber length [m]
L'	lower limit of the decision variables

L''	upper limit of the decision variables
N	compression stages
N_c	DDF mean
P	permeability [barrer]
p	pressure [bar]
Q	heat duty [W]
R	reflux stream
r	reflux stream DDF
T	temperature [K]
t	set of model constraints
v	vector of model decision variables
W	compression duty [W]
x	liquid mole fraction [-]
y	vapor mole fraction [-]
z	hollow fiber axial dimension [m]

Greek letter

α	selectivity [-]

δ active layer thickness [m]

γ permeate-to-feed pressure ratio [-]

η compressors efficiency [-]

λ C_p/C_v ratio [-]

μ molar flowrate [mol h^{-1}]

Θ grouped parameter [-]

σ standard deviation [-]

Superscript / subscript

B bottoms stream

C_3H_6 propylene

C_3H_8 propane

D distillate stream

F feed side

I column tray

j component

k column tray

P permeate side

1. Introduction

The use of ethylene and propylene as main building blocks for a wide number of essential chemicals turns them into the most important feedstocks of the petrochemical industry. The separation of these light olefins from their homologous paraffin entails a costly high pressure or cryogenic distillation with a prominent contribution to the worldwide energy consumption [1]. Although major efforts have been carried out to develop alternative separation processes, mainly enhanced distillations [2] and physical/chemical adsorptions [3,4], none of them have succeeded in replacing traditional distillation.

Process intensification by means of membrane technology is one of the most promising strategies to overcome this handicap, performing the separation at mild temperature and pressure conditions using modular and compact equipment [5]. A characteristic feature of membrane materials is the existing trade-off between the amount of gas that passes though the film (i.e. permeability) and the selectivity towards the desired gaseous species. In addition, this effect can be a decisive factor for further industrial application.

Dense polymeric membranes, based exclusively on solution-diffusion transport, offer poor performance in terms of selectivity, and their potential industrial application may be found in the recovery of unreacted olefin after polymerization, where selectivity values of 3-5 may be adequate [6,7]. The search for better separation capabilities has led to the development of new materials that excel in olefin/paraffin separation applications. Carbon molecular sieves prepared through pyrolysis of polymer precursors display a complex morphology combining ultramicropores and micropores, which are responsible for the molecular sieving and the solubility, respectively. These show

propane/propylene selectivity values up to 50 and permeability values around 20 barrer [8–10]. Zeolitic imidazolate framework (ZIF) membranes present a structure built upon metals with tetrahedral coordination geometries interlinked with imidazolate ligands, which separates the mixture based on the differences in diffusivity through the pore system. These ceramic membranes perform selectivity values as high as 70 with a permeability ranging between 100 and 400 barrer [11–13]. Finally, facilitated transport membranes make use of silver cations as carrier, selectively transporting the olefin through the membrane and, reaching a selectivity higher than 100 with permeability values typically surpassing 1000 barrer [14–16]. Additionally, the use of ionic liquids and silver nanoparticles to enhance the performance and carrier stability has been reported to produce favorable effects [17,18]. These permeation results outperform the propylene/propane upper bound of dense polymers [19,20]. However, it has been demonstrated by Park et al. that, "designing materials with selectivity values much greater than the pressure ratio yields little or no improvement in product purity" [21].

Besides material separation performance, another critical aspect is the membrane configuration. Among the possible configurations, hollow fiber membranes are widely recognized for their adequacy in industrial gas separations, offering high packing density and energy efficiency [22]. In this regard, carbon molecular sieves, ZIF's and facilitated transport membranes can be processed to produce hollow fibers [8,23].

Whilst the complete replacement of the conventional distillation would require materials that exceed the current upper-bound, state-of-the-art membranes could be effectively implemented in a hybrid process [1,24,25]. A hybrid process is defined as a process array combining different unit operations, which are interlinked and optimized to accomplish a predefined task [26]. It is worth noting that the hybrid membrane/distillation concept comprises a limited number of arrangements [27,28]. All

these alternatives have been previously reported in the literature by Moganti et al. [29], and Pressley and Ng [24].

The design of a membrane/distillation hybrid process involves solving an optimization problem, driven by the existing compromise between the membrane total cost and the column operating expenses. Although it is conceivable to expand the optimization problem to all possible configurations using a complex superstructure, the limited number of different arrangements allows optimizing each configuration independently in a more efficient manner [30]. Following this strategy, Caballero et al. [30] developed a model to optimize the ethane/ethylene separation using the parallel arrangement (i.e. feeding the membrane with an intermediate column product and then feeding back the column with the permeate and retentate streams); likewise, Kookos [31] optimized the same configuration for propane/propylene mixtures.

Recently, Wessling et al. [32] proposed the use of upper-bound membrane properties coupled with process modeling to find the optimal combination of permeability and selectivity for gas separation. In this work, we extend this concept to hybrid systems by developing an optimization model of a membrane/distillation hybrid process for propylene/propane separation. A model of the membrane module is proposed considering a co-current hollow fiber configuration. The distillation column is modeled formulating the MESH equations (material balance, equilibrium, summation and enthalpy balance), and for tray optimization we avoid the use of binary variables, and the subsequent MINLP problem, by using the Distributed Stream-Tray Optimization Method (DSTO) developed by Lang and Biegler [33].

This optimization is intended as a proof of concept of the state-of-the-art membrane materials, introducing the selectivity and permeability reported values and comparing

the total operating costs resulting from the implementation of a hybrid process with those of the base case distillation.

2. Optimization Methodology

2.1. Problem Statement

In this work, the problem can be formulated as: given the head product of an industrial depropanizer, assess the potential capability of state-of-the-art membrane materials to reduce the economic impact of the gas separation by optimizing a hybrid hollow fiber/distillation separation system. As the hybrid system is highly suitable for retrofitting existing distillation columns, the conventional distillation will be taken as reference for the number of equilibrium stages.

2.2. Hollow fiber membrane model

In the proposed process configuration the membrane module receives the depropanizer head product. Although this stream is typically condensed and fed into the next distillation column [34], we will assume that the condenser would be partially by-passed if a hybrid process were to be implemented. In this way, a vapor stream is available to be directly introduced into the hollow fibers module.

The mathematical description of the membrane unit considers the following assumptions:

- The module operates isothermally and in the steady state.
- The feed stream is introduced in the shell side of the fibers, with the permeate circulating in the lumen side.
- The feed and permeate streams flow in a co-current configuration.
- Plug-flow in both sides is assumed.
- The total pressure in the feed and permeate sides are kept constant as operating conditions.

- There is no pressure drop due to fluid dynamics, the only pressure gradient is the transmembrane pressure.
- The gas permeability is a material constant.

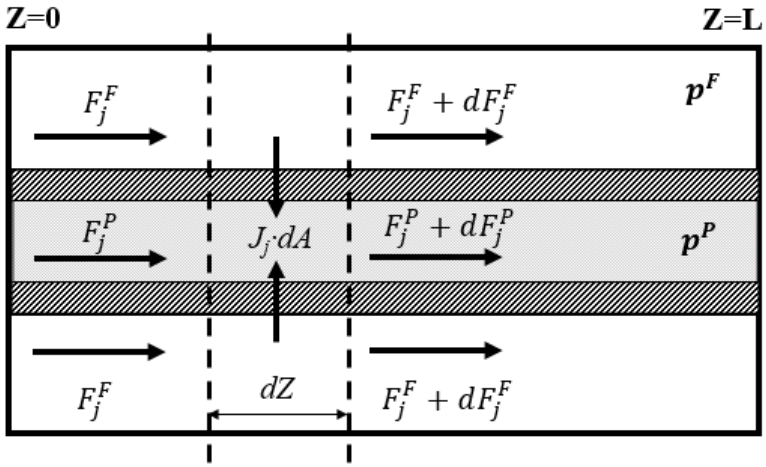

Fig 1. Schematic diagram of the hollow fibers module.

Figure 1 shows a schematic diagram of the hollow fibers module. The mass balances for component *j* in the feed and permeate sides are as follows:

$$dF_j^F(z) = -J_j(z) \cdot dA \qquad (1)$$

$$dF_j^P(z) = J_j(z) \cdot dA \qquad (2)$$

where F_j is the molar flowrate of component *j*, and dA is the fiber wall area differential element. Given that the reported permeability can be considered as a normalized flux, we revert this conversion to calculate the permeation flux through the active layer, as outlined by the solution-diffusion theory [35]:

$$J_j(z) = \frac{\mathrm{P}_j}{\delta} \cdot \left[p_j^F(z) - p_j^P(z) \right] \quad (3)$$

where P_j is the permeability of component *j*, δ is the thickness of the active layer and p_j^F and p_j^P are feed and permeate partial pressures of component *j*, respectively. This should be interpreted as an approximation to homogenize the calculation method when evaluating membrane materials that perform a variety of transport mechanisms. The following dimensionless variables are defined:

$$\bar{z} = \frac{z}{L} \qquad \bar{z} \in [0,1] \quad (4)$$

$$\gamma = \frac{p^P}{p^F} \qquad \gamma \in [0,1] \quad (5)$$

$$\overline{F_j}(z) = \frac{F_j(z)}{F_T^F(z=0)} \qquad \overline{F_j} \in [0,1] \quad (6)$$

$$x_j(z) = \frac{F_j^F(z)}{\sum F_j^F(z)} \qquad x_j \in [0,1] \quad (7)$$

$$y_j(z) = \frac{F_j^P(z)}{\sum F_j^P(z)} \qquad y_j \in [0,1] \quad (8)$$

which stand for feed and permeate mole fraction, dimensionless axial length, permeate-to-feed pressure ratio and dimensionless molar flowrate, respectively; *L* is the fiber length. In addition, a grouped parameter is defined:

$$\Theta_j = \frac{A \cdot \mathrm{P}_j \cdot p^F}{\delta \cdot F_{T,z=0}^F} \quad (9)$$

where A is the total membrane area. Rearranging terms, the mass balances can be rewritten as:

$$\frac{d\overline{F_j^F}}{d\bar{z}} = -\Theta_j \cdot \left(x_j - \gamma y_j\right) \tag{10}$$

$$\frac{d\overline{F_j^P}}{d\bar{z}} = \Theta_j \cdot \left(x_j - \gamma y_j\right) \tag{11}$$

$$\left.\overline{F_j^F}\right|_{\bar{z}=0} = 1 \tag{12}$$

$$\left.\overline{F_j^P}\right|_{\bar{z}=0} = 0 \tag{13}$$

These ordinary differential equations (ODEs) (Eqs. 10-13) are discretized using implicit Runge-Kutta collocation methods and solved as algebraic equations.

2.3. Distillation model.

For the distillation column, the model is taken from the work of Lang and Biegler [33]. A complete description of the mathematical development can be found in the original manuscript, here we provide a brief overview. In order to avoid discrete decision variables, the model uses differentiable distribution functions (DFF) for the feed streams, reflux stream and intermediate product streams (if present), in the form:

$$d_i = \frac{\exp\left[-\left(\frac{i-N_c}{\sigma}\right)^2\right]}{\sum_k \exp\left[-\left(\frac{k-N_c}{\sigma}\right)^2\right]} \quad i,k \in I \tag{14}$$

which corresponds to the discretization of a Gaussian distribution with mean N_c and standard deviation σ. Thus, using DDFs, the feed and reflux streams can be distributed to all trays:

$$E_i = E \cdot e_i \tag{15}$$

$$R_i = R \cdot r_i \tag{16}$$

where E_i and R_i are the feed and reflux flowrates entering into the *i*-th tray, e_i and r_i are the corresponding differentiable distribution functions and E and R are the total feed and reflux streams, respectively. Once the feed and reflux streams are defined through a DDF, the model uses the conventional MESH equations (material balances, equilibrium, summation and enthalpy balances) to formulate the distillation model. As described in [33] the model is also capable of calculating the number of trays by relaxing the equilibrium equations in the MESH equations so that the liquid phase disappears. This modification of the MESH equations allows dry trays to appear without pressure drop in the non-existing trays above the reflux insertion point. The optimization model then chooses the column operation with the optimal number of dry trays, which translates to the optimum number of trays required. Figure 2 depicts an overview of the modelling strategy.

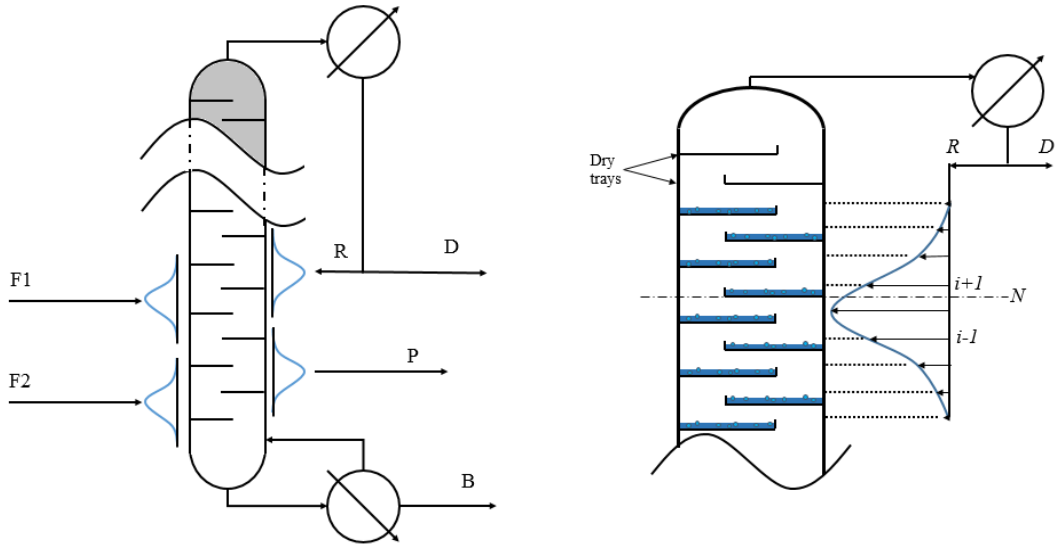

Fig 2. Schematic diagram of the Distributed Stream-Tray Optimization Method (DSTO) and detail of reflux stream DDF.

The vapor-liquid equilibrium has been introduced using the K-value charts for C_3 mixtures [36]. These charts are constructed upon experimental data, later displayed in nomograms. To allow its implementation in computer calculations, a corresponding states type approach has been reported in the bibliography [37]. This approach considers the equilibrium constant value as a function of pressure and temperature exclusively, neglecting the effects of composition. This assumption is valid for propane/propylene mixtures at the pressure and temperature range covered in this study.

2.4. Distillation Benchmark

To quantify the potential economic savings, we establish the conventional distillation as base case. The feed stream consist of 360 kmol/h of a liquid propane/propylene equimolar mixture at 323 K and 20.27 bar. The product specifications are 0.995 propylene mole fraction in the distillate stream (i.e. polymer grade) and 0.95 propane mole fraction in the bottoms stream. The column has 135 equilibrium stages including the reboiler and condenser with a total reflux ratio of 14.9. The base case distillation

reflux ratio has been calculated using the same vapor-liquid equilibrium method discussed before. In this way we remove any bias caused by the use of different thermodynamic methods when comparing results. More detailed information about the base case can be found in Table 1.

Table 1. Distillation parameters

Parameter	Value
Feed temperature (K)	323
Feed pressure (bar)	20.27
Feed flowrate (kmol h^{-1})	360
Feed composition (C_3H_6 mol frac.)	0.50
Feed tray[a]	51
Distillation column number of stages	135
Reflux ratio	14.91
Reboiler duty (kW)	15128
Condenser duty (kW)	14169
Dist. temperature (K)	320.05
Dist. pressure (bar)	19.05
Dist. flowrate (kmol h^{-1})	171.43
Dist. composition (C_3H_6 mol frac.)	0.995
Bott. temperature (K)	331.57
Bott. pressure (bar)	20.41
Bott. flowrate (kmol h^{-1})	188.57
Bott. composition (C_3H_6 mol frac.)	0.05

[a] Column trays are numbered from bottom to top.

2.5. State-of-the-art membrane materials

We propose a selection of membrane materials to represent the current industrially attractive possibilities for a hybrid process. In the field of carbon molecular sieves, Ma et al. [38] recently reported a high performance membrane prepared *via* pyrolysis of defect-free polymers on a γ-alumina support. In this way, they managed to synthesize CMS membranes with an active layer of 0.3 μm, yielding propylene permeances around 42 GPU with a selectivity of 23.

Regarding ZIF membranes, Pan et al. [39] reported a ZIF-8 membrane performing propylene permeances up to 90 GPU and selectivity values around 50. These

membranes were synthesized by hydrothermal seeded growth on α-alumina supports, and resulted in an effective layer thickness of 2.2 μm. Using a heteroepitaxial growth method, Kwon et al. [40] created a selective membrane displaying successive zeolitic selective layers on α-alumina supports. They achieved a ZIF-8/ZIF-67/ZIF-8 structure performing a propylene permeance of 110 GPU and selectivity values around 210.

Recently, our research group has reported facilitated transport membranes showing a propylene permeance up to 40 GPU with a selectivity of 150 [15]. This membrane was synthesized incorporating silver cations in a PVDF-HFP/$BMImBF_4$ polymer/ionic liquid matrix. The selective coordination of propylene with the silver cations is responsible for the high olefin solubility, while the dense nature of the fluoropolymer limits the paraffin transport.

Furthermore, two well studied membranes, a polyimide [41] and an cellulosic membrane [42] have been introduced in this study as exponents of previous generations of materials for comparison purposes. Table 2 summarizes the selected membranes features.

Finally, the permeability-selectivity trade-off exhibited by membrane materials has been assessed, introducing an updated trade-off expression in the optimization model. In this way, a wider insight into state-of-the-art membrane performance can be provided.

Table 2. Separation performance of the selected membranes

Membrane	C_3H_6 Permeance (GPU[a])	C_3H_6 Selectivity	Source
CMS	42	23	[38]
ZIF-8	90	50	[39]
ZIF-8/ZIF-67/ZIF-8	111	210	[40]
PVDF-HFP/$BMImBF_4$/$AgBF_4$	40	150	[15]
6FDA-TeMPD	37[b]	8.6	[41]
EC	7	7.0	[42]

[a] 1 GPU=3.35×10^{-10} mol/m^2 Pa s

[b] Calculated from reported permeability assuming 1 μm thickness

2.6. Hybrid process optimization

The hybrid process flowsheet is displayed in Figure 3. Briefly, the propane/propylene gaseous mixture coming from the previous depropanizer unit is fed into the hollow fiber module. Then, the resultant retentate and permeate streams are recompressed and introduced in the distillation column to perform the final refining step. In order to assess the membrane performance when retrofitting the existing process, and as far as only operating costs are evaluated, the same number of equilibrium stages of the benchmark distillation column is considered in the hybrid configuration. In addition, the base case distillate and bottoms purities are taken as the hybrid process constraints. Heat integration strategies are not considered in the present work, as they may depend upon the configuration of each specific production plant. The process parameters are summarized in Table 3.

Table 3. Hybrid process parameters

Parameter	Value
Feed temperature (K)	325
Feed pressure (bar)	18
Feed flowrate (kmol h^{-1})	360
Feed composition (C_3H_6 mol frac.)	0.50
Membrane feed side pressure (bar)	18
Membrane permeate side pressure (bar)	1
Distillation column number of stages	135
Distillate purity, $x^{D}_{C_3H_6,min}$ (mol%)	$\geq$ 99.5
Bottoms purity, $x^{B}_{C_3H_8,min}$ (mol%)	$\geq$ 95.0

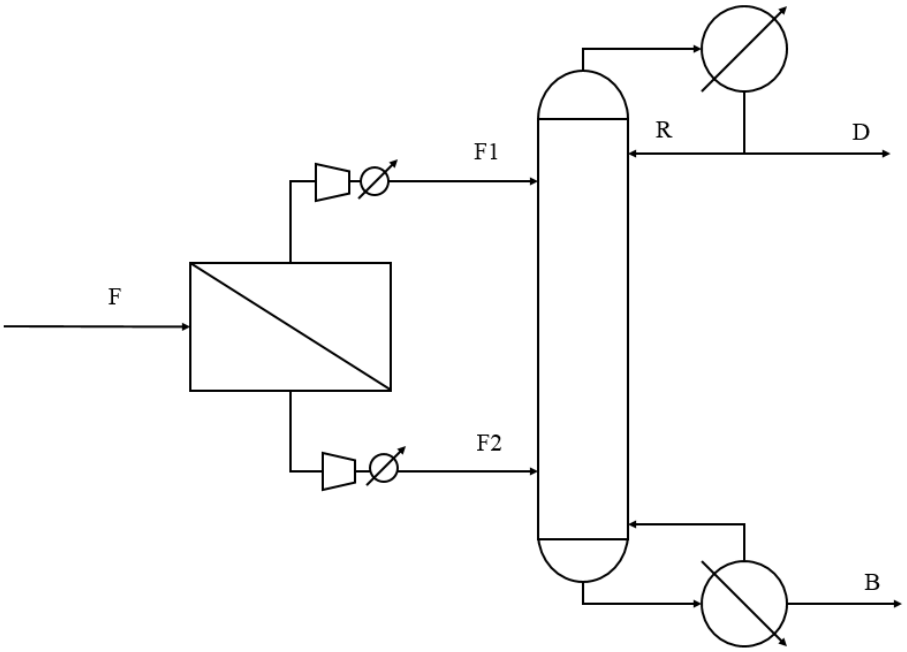

Fig 3. Schematic diagram of the hybrid process.

In this work, the optimization objective aims to minimize the total operating costs. Here we include:

- Membrane depreciation.
- Permeate and retentate recompression.
- Reboiler and condenser duties.

The membrane depreciation can be easily calculated as the membrane cost divided by the membrane lifetime, thus obtaining the annualized cost. The compressors duty can be calculated as follows:

$$W = \frac{\mu N}{\eta}\left(\frac{\lambda}{\lambda-1}\right)RT_{feed}\left[\left(\frac{p_N}{p_{feed}}\right)^{\frac{\lambda-1}{\lambda N}}-1\right] \qquad (17)$$

where μ is the molar flowrate, N is the number of compression stages, η is the compressor efficiency, λ is the C_p/C_v ratio of the compressed gas, and p_N is the outlet pressure. The reboiler and condenser duties are calculated using the following expression:

$$Q = \mu \sum_j x_j \, \Delta H_{vap,j} \qquad (18)$$

where x_j and $\Delta H_{vap,j}$ are the mole fraction and enthalpy of vaporization of component *j* in the stream, respectively.

The compression and heat exchange duties are further converted to annualized expenses using the respective utilities price. Table 4 shows the parameters regarding the economic calculations.

Table 4. Process parameters for the economic estimation

Parameter	Value
Membrane unitary cost ($ m^{-2})	20
Membrane lifetime (year)	2
Post-compression pressure (bar)	20.27
Post-compression temperature (K)	323
Permeate compressor number of stages	3
Retentate compressor number of stages	1
Compression efficiency	0.72
$\gamma = C_p/C_v$	1.15
Energy cost ($ kWh^{-1})	7.70E-02
Steam@150psi cost ($ mol^{-1})	3.23E-04
Cooling water cost ($ mol^{-1})	5.70E-07
Plant service factor	0.904

To conclude, the objective function can be formulated in the standard form as:

$$\begin{aligned} &\textit{Minimize } TOC(v) \\ &s.t. \\ &\quad h(v) = 0 \\ &\quad t(v) \geq 0 \\ &\quad L' \leq v \leq L'' \end{aligned} \qquad (19)$$

where TOC is the total annualized operating cost, v is the vector of model decision variables, $h(v)$ is the set of model algebraic equations, $t(v)$ is the set of model constraints (Eqs. 20-21) and L' and L'' are the lower and upper limits of the decision variables, respectively.

$$x^{D}_{C_3H_6} \geq x^{D}_{C_3H_6,min} \qquad (20)$$

$$x^{B}_{C_3H_8} \geq x^{B}_{C_3H_8,min} \qquad (21)$$

The model has been implemented in the General Algebraic Modelling System (GAMS) and solved using the multistart heuristic algorithm OQNLP on a 3.40 GHz Intel® Core™ i7-3770 processor. The GAMS code is available as electronic supplementary information. CONOPT has been used as local NLP solver for OQNLP with a time limit of 3000 seconds and a maximum of 3000 trial points and 3000 CONOPT calls. The number of single equations and single variables, which depend on the case study, are displayed in Table 5.

Table 5. Models statistics

	BCD[a]	HP[b]	HP-OMP[c]
Number of single equations	4061	4669	4671
Number of single variables	4335	4945	4948

[a] Base Case Distillation
[b] Hybrid Process
[c] Hybrid Process- Optimal Membrane Properties

Once the solver is run, it provides:

- The minimal operating expenses (and the partial contributions).
- The optimal membrane area.
- The optimal reflux ratio.
- The optimal feed tray locations.

3. Results and discussion

In this section, we first present the results obtained for the hybrid configuration with the selected membrane materials. Next, the current membrane upper bound is introduced in the model to study the desirable permeability/selectivity combination of a hypothetically optimal membrane material. Additionally, the impact of the membrane cost on the economic evaluation is assessed.

3.1. State-of-the-art membranes optimization results

Table 6 displays the resultant membrane area, reflux ratio and potential savings derived from the implementation of each membrane in a hybrid configuration. The highly permeable and highly selective ZIFs, CMS and facilitated transport membranes (**A-D**) can potentially reduce the operating expenses by around 30 to 55%. In addition, advanced polyimides, as 6FDA-TeMPD (**E**), which provide high permeance but moderate selectivity, are still capable of reducing the total operating costs by 18%. Finally, the cellulosic membrane (**F**), due to its low permeance and selectivity, achieves a TOC reduction of around 10%.

Table 6. Optimization results

ID	Membrane	C_3H_6 Permeance (GPU)	Selectivity	Area ($x10^3$ m^2)	Reflux	TOC (MM$/y)	Savings (%)
-	None	-	-	-	14.9	4.05	0.0
A	ZIF8 / ZIF67/ZIF8	111	209	2.8	4.5	1.78	56.2
B	PVDF-HFP/$AgBF_4$/BMImBF_4	40	150	7.4	5.3	2.02	50.3
C	ZIF 8	91	50	2.9	7.4	2.50	38.3
D	6FDA-based polyimide CMS	42	23	5.8	8.7	2.87	29.2
E	6FDA-TeMPD	37	8.9	5.3	10.5	3.34	17.6

F	EC	6	7.0	23.2	11.2	3.65	9.9

The TOC reduction due to the implementation of a hollow fiber module in series is clearly related to the decrease in the required reflux ratio for a given product quality. Although the reboiler and condenser duties are very similar, the use of steam requires that more than 95% of the base case operating costs are generated by the reboiler. Figure 4 unfolds the total operating expenses for each case. As expected, the membrane module helps reduce the required reflux ratio, decreasing the steam supply to the reboiler and its associated cost. It is worth noting that, despite this reduction, the reboiler operating cost is still the largest contribution to the total operating costs, while the condenser and retentate compressor operating costs are almost negligible.

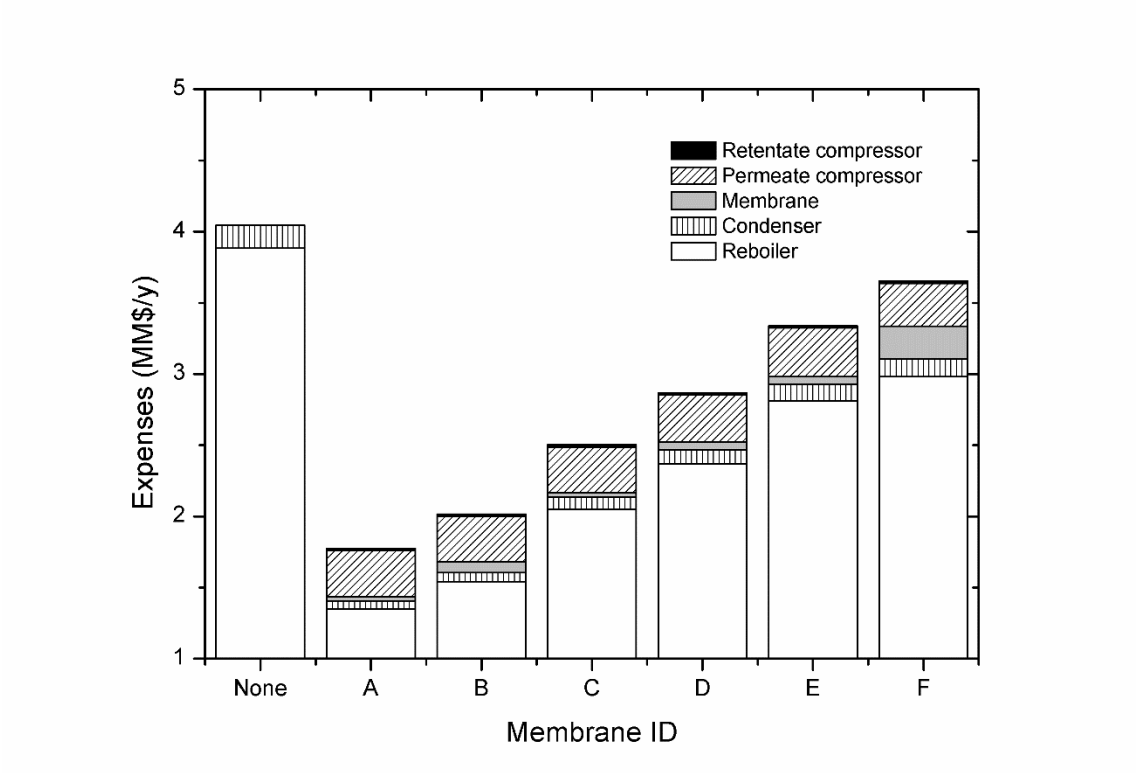

Fig 4. Disaggregated operating costs for each case. A-F defined in Table 6.

Focusing on the intermediate streams (F1 and F2 in Figure 3), it is noticeable how the optimal solution comprises, in all cases, approximately the same flowrates, and the total savings are eventually determined by the purity achieved in these streams as can be seen in Table 7. In this regard, the optimal membrane area for case **B** is higher than that of case **D**. Though both have the same propylene permeance, the first is far more selective. Here, the extra cost is offset by the purity reached in the permeate stream. Comparing membranes with similar selectivity (**E** and **F**), we observe the strong dependence of the optimal required area on the membrane permeance.

Table 7. Intermediate streams results.

ID	Membrane	F1 flowrate (kmol/h)	F2 flowrate (kmol/h)	F1 C_3H_6 purity (kmol/h)	F2 C_3H_6 purity (kmol/h)	F1 feed tray[a]	F2 feed tray[a]	Savings (%)
A	ZIF8 / ZIF67/ZIF 8	159	201	0.985	0.115	108	19	56.2
B	PVDF-HFP/AgBF$_4$/BMImBF$_4$	157	203	0.981	0.127	102	19	50.3
C	ZIF 8	158	202	0.950	0.149	83	18	38.3
D	6FDA-based polyimide	161	199	0.906	0.170	75	19	29.2
E	CMS 6FDA-TeMPD	167	193	0.815	0.227	70	24	17.6
F	EC	147	213	0.806	0.289	74	30	9.9

[a] Column trays are numbered from bottom to top.

Since the hybrid configuration may become uncompetitive compared to the conventional distillation depending on the membrane unitary cost, it is advisable to perform a sensitivity analysis of the optimum solutions. Figure 5 displays the TOC variation for each membrane with increasing membrane prices up to 200\$/m^2. In all

cases, with the exception of the cellulosic membrane, the optimal configuration does not vary significantly, and the resultant TOC increase is proportional to the optimal membrane area. On the other hand, the cellulosic membrane hybrid configuration, due to the large area required, is not suitable for replacing the base case distillation when the membrane cost exceeds ~100\$/m^2, and consequently, the membrane module has been removed during the optimization run.

This analysis reveals a remarkable range of suitability for medium to high performance membrane materials when implemented in a hybrid configuration, regarding the membrane production cost.

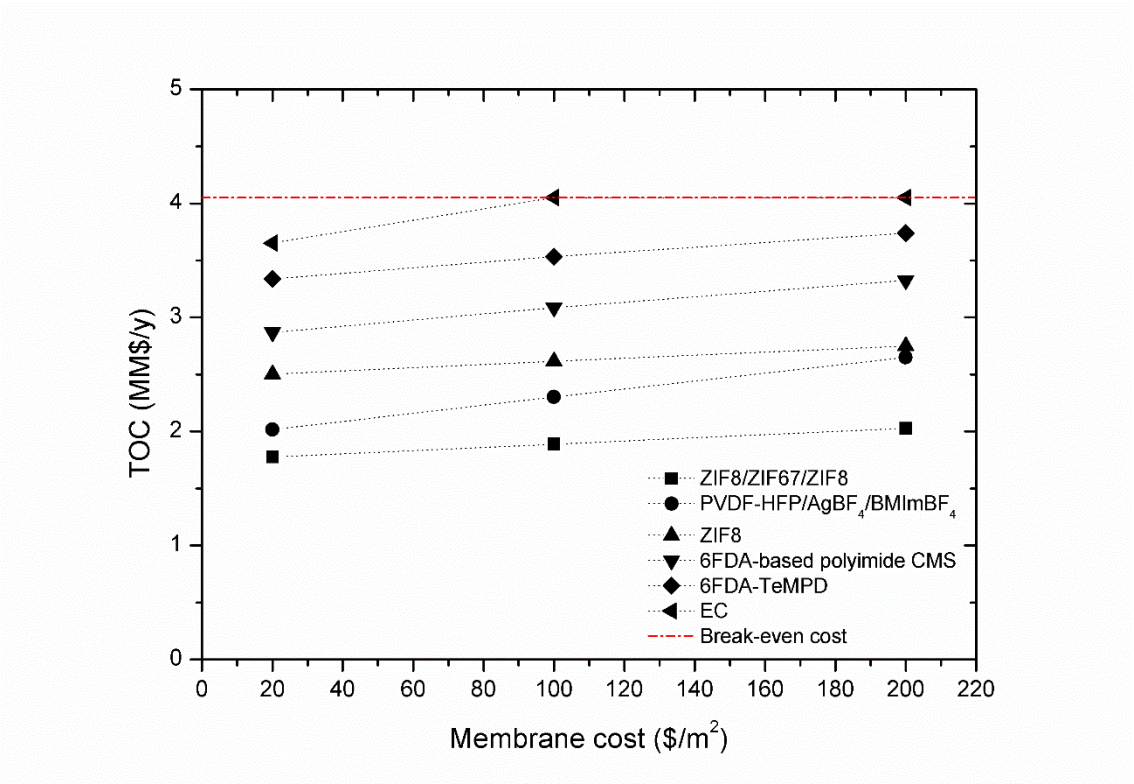

Fig 5. Effect of the membrane cost on optimal TOC for the studied membranes.

3.2. Upper-bound role in the hybrid configuration

An interesting point when dealing with membranes is the trade-off existing between selectivity and gas permeability, which is limited by the upper-bound in the Robeson plot. By introducing the Robeson plot upper-bound expression in the optimization model we can explore the optimal permeability and selectivity values of a hypothetically optimal membrane material, given the membranes state-of-the art [30,31]. Figure 6 represents an updated Robeson plot for propane/propylene mixtures.

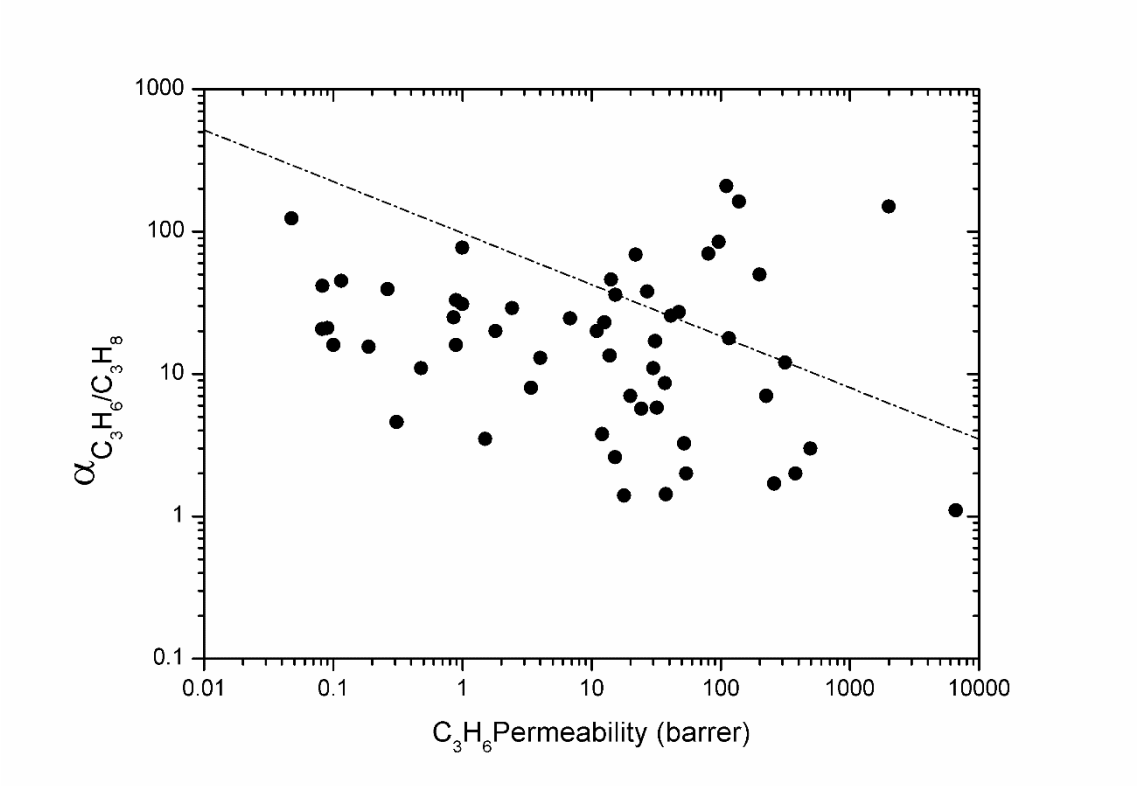

Fig 6. Robeson plot for propane/propylene separation membranes displaying the upper-bound.

The corresponding mathematical expression is:

$$\alpha_{C_3H_6/C_3H_8} = 97.51\, P_{C_3H_6}^{-0.362} \qquad (22)$$

This updated upper-bound is slightly displaced towards the high-performance region compared to the previous version reported by Burns and Koros [19], as a result of the

continuous research in membrane materials over the recent years. In this section we will evaluate the membrane productivity in terms of permeability instead of permeance, due to the nature of the Robeson plot, which is intended to compare materials and not specific membrane morphologies.

Once the upper-bound is introduced in the optimization problem, in addition to membrane area, reflux ratio and stream locations, the program also provides the optimal balance between permeability and selectivity. An active layer thickness of 1μm has been assumed, as this is a typical value in the hollow fiber manufacture. The same hybrid process parameters considered in the previous discussion have been used for this section (see Table 3). The results obtained in this section are summarized in Table 8.

Table 8. Upper-bound optimization results

	Membrane cost ($/m^2)		
	20	100	200
Propylene permeability (barrer[a])	16	74	134
Propylene selectivity	36	21	17
Membrane area (x10^3 m^2)	15.0	3.1	1.6
F1 flowrate (kmol/h)	155	158	157
F2 flowrate (kmol/h)	205	202	203
F1 C_3H_6 purity	0.937	0.901	0.885
F2 C_3H_6 purity	0.171	0.187	0.203
F1 feed tray[b]	82	76	76
F2 feed tray[b]	21	21	23
Reflux ratio	8.0	8.9	9.3
TOC (MM$/y)	2.77	3.02	3.13
Savings (%)	31.5	25.5	22.8

[a] 1 barrer=3.348x10^{-16} mol m/m^2 Pa s
[b] Column trays are numbered from bottom to top.

The optimal solution involves, in this case, very similar intermediate flowrates to those discussed in the previous section (see Table 7), and the potential reflux reduction is again determined by the purity of theses streams (F1 and F2 in Figure 3). It is worth

noting the strong influence of the membrane cost on the optimal permeability/selectivity trade-off. As the membrane cost weight on the objective function increases, the membrane tends to increase the permeability at the expense of selectivity. In the most unfavorable case (i.e. 200\$/m^2) the membrane is highly permeable and the selectivity falls to a value closer to the pressure ratio, which allows a prominent decrease in the required area while still maintaining an adequate permeate purity. These results are in good agreement with Huang et al. [43] findings on the pressure ratio-selectivity relation: "High permeance membranes are always good, but the optimum membrane selectivity depends on the process and the operating conditions, particularly the pressure ratio". Increasing the membrane selectivity far beyond the industrially suitable pressure ratio produces minor increments in the product purity at the expense of larger membrane areas, as the process enters in the pressure ratio-limited region.

Comparing with the real membranes selected for this study, the carbon molecular sieve (membrane **D**) would be the option of choice, given the conservative upper-bound considered in Eq. 22, which is below the performance of membranes **A**, **B** and **C**. This gives an idea of the state-of-the-art membrane materials performance for process intensification when implemented in a hybrid configuration.

Conclusions

Membrane technology offers remarkable opportunities to intensify the olefin/paraffin separation process when implemented in hybrid systems along with the conventional distillation. In this work, the optimization of a membrane/distillation hybrid process with state-of-the-art membranes yielded total operating cost savings of 10-50% compared with the distillation benchmark.

The evaluation of the Robeson plot upper-bound reveals the importance of the operating conditions when it comes to select the most suitable membrane. Especially, the pressure ratio may limit the advantages of highly selective membranes. In this regard, membrane researchers should consider the particularities of each specific application in order to tailor the membrane properties accordingly.

Acknowledgements

Financial support from the Spanish Ministry of Science under the projects CTQ2015-66078-R and CTQ2016-75158-R (MINECO, Spain-FEDER 2014–2020) is gratefully acknowledged. Raúl Zarca also thanks the Universidad de Cantabria for a postgraduate fellowship.

References

1. Sholl, D. S. & Lively, R. P. Seven chemical separations to change the world. *Nature* **532,** 435–437 (2016).

2. Kumar, R., Prausnitz, J. M. & King, C. J. Process design considerations for extractive distillation: separation of propylene-propane. in *Extractive and Azeotropic Distillation* (ed. Dimitrios P. Tassios) 16–34 (1972).

3. Shu, C. M., Kulvaranon, S., Findley, M. E. & Liapis, A. I. Experimental and computational studies on propane-propylene separation by adsorption and

variable-temperature stepwise desorption. *Sep. Technol.* **1,** 18–28 (1990).

4. Padin, J., Rege, S. U., Yang, R. T. & Cheng, L. S. Molecular sieve sorbents for kinetic separation of propane/propylene. *Chem. Eng. Sci.* **55,** 4525–4535 (2000).

5. Charpentier, J. C. In the frame of globalization and sustainability, process intensification, a path to the future of chemical and process engineering (molecules into money). *Chem. Eng. J.* **134,** 84–92 (2007).

6. Baker, R. W. Future directions of membrane gas separation technology. *Ind. Eng. Chem. Res.* **41,** 1393–1411 (2002).

7. Faiz, R. & Li, K. Polymeric membranes for light olefin/paraffin separation. *Desalination* **287,** 82–97 (2012).

8. Xu, L. *et al.* Olefins-selective asymmetric carbon molecular sieve hollow fiber membranes for hybrid membrane-distillation processes for olefin/paraffin separations. *J. Memb. Sci.* **423–424,** 314–323 (2012).

9. Askari, M. & Chung, T.-S. Natural gas purification and olefin/paraffin separation using thermal cross-linkable co-polyimide/ZIF-8 mixed matrix membranes. *J. Memb. Sci.* **444,** 173–183 (2013).

10. Liu, J. *et al.* A new carbon molecular sieve for propylene/propane separations. *Carbon.* **85,** 201–211 (2015).

11. Li, K. *et al.* Zeolitic imidazolate frameworks for kinetic separation of propane and propene. *J. Am. Chem. Soc.* **131,** 10368–10369 (2009).

12. Demir, B. & Ahunbay, M. G. Propane/propylene separation in ion-exchanged zeolite-like metal organic frameworks. *Microporous Mesoporous Mater.* **198,** 185–193 (2014).

13. Kwon, H. T. & Jeong, H. K. Improving propylene/propane separation performance of Zeolitic-imidazolate framework ZIF-8 membranes. *Chem. Eng. Sci.* **124,** 20–26 (2015).

14. Fallanza, M., Ortiz, A., Gorri, D. & Ortiz, I. Polymer-ionic liquid composite membranes for propane/propylene separation by facilitated transport. *J. Memb. Sci.* **444,** 164–172 (2013).

15. Zarca, R., Ortiz, A., Gorri, D. & Ortiz, I. Generalized predictive modeling for facilitated transport membranes accounting for fixed and mobile carriers. *J. Memb. Sci.* **542,** 168–176 (2017).

16. Ravanchi, M. T., Kaghazchi, T. & Kargari, A. Supported liquid membrane separation of propylene-propane mixtures using a metal ion carrier. *Desalination* **250,** 130–135 (2010).

17. Kang S.W., *et al.* Effect of the polarity of silver nanoparticles induced by ionic liquids on facilitated transport for the separation of propylene/propane mixtures, J. Memb. Sci. **322,** 281–285 (2008).

18 Jeong S., Kang S.W. Effect of Ag_2O nanoparticles on long-term stable

polymer/AgBF4/Al(NO3)3complex membranes for olefin/paraffin separation, Chem. Eng. J. **327,** 500–504 (2017).

19. Burns, R. L. & Koros, W. J. Defining the challenges for C3H6/C3H8 separation using polymeric membranes. *J. Memb. Sci.* **211,** 299–309 (2003).

20. Robeson, L. M. The upper bound revisited. *J. Memb. Sci.* **320,** 390–400 (2008).

21. Park, H. B., Kamcev, J., Robeson, L. M., Elimelech, M. & Freeman, B. D. Maximizing the right stuff: The trade-off between membrane permeability and selectivity. *Science.* **356,** 1138–1148 (2017).

22. Nymeijer, D. C., Visser, T., Assen, R. & Wessling, M. Composite hollow fiber gas-liquid membrane contactors for olefin/paraffin separation. *Sep. Purif. Technol.* **37,** 209–220 (2004).

23. Brown, A. J. *et al.* Interfacial microfluidic processing of metal-organic framework hollow fiber membranes. *Science.* **345,** 72–75 (2014).

24. Pressly, T. G. & Ng, K. M. A Break-Even Analysis of Distillation-Membrane Hybrids. *AIChE J.* **44,** 93–105 (1998).

25. Norkobilov, A., Gorri, D. & Ortiz, I. Comparative study of conventional, reactive-distillation and pervaporation integrated hybrid process for ethyl tert-butyl ether production. *Chem. Eng. Process. Process Intensif.* **122,** 434–446 (2017).

26. Lipnizki, F., Field, R. W. & Ten, P.-K. Pervaporation-based hybrid process: a review of process design, applications and economics. *J. Memb. Sci.* **153,** 183–210 (1999).

27. Stephan, W., Noble, R. D. & Koval, C. A. Design methodology for a membrane/distillation column hybrid process. *J. Memb. Sci.* **99,** 259–272 (1995).

28. Pettersen, T., Argo, A., Noble, R. D. & Koval, C. A. Design of combined membrane and distillation processes. *Sep. Technol.* **6,** 175–187 (1996).

29. Moganti, S., Noble, R. D. & Koval, C. A. Analysis of a membrane/distillation column hydrid process. *J. Memb. Sci.* **93,** 31–44 (1994).

30. Caballero, J. A. *et al.* Design of hybrid distillation - vapor membrane separation systems. *Ind. Eng. Chem. Res.* **48,** 9151–9162 (2009).

31. Kookos, I. K. Optimal design of membrane/distillation column hybrid processes. *Ind. Eng. Chem. Res.* **42,** 1731–1738 (2003).

32. Ohs, B., Lohaus, J. & Wessling, M. Optimization of membrane based nitrogen removal from natural gas. *J. Memb. Sci.* **498,** 291–301 (2016).

33. Lang, Y. D. & Biegler, L. T. Distributed stream method for tray optimization. *AIChE J.* **48,** 582–595 (2002).

34. Luyben, W. L. Dynamic simulation of flooded condensers. *Chem. Eng. Res. Des.* **118,** 12–20 (2017).

35. Wijmans, J. G. & Baker, R. W. The solution-diffusion model: a review. *J. Memb. Sci.* **107,** 1–21 (1995).

36. Scheibel, E. G. & Jenny, F. J. Nomographs for Enthalpies of Pure Hydrocarbons and Their Mixtures. *Ind. Eng. Chem.* **37,** 990–995 (1945).

37. Dimitrios Tassios, *Applied Chemical Engineering Thermodynamics*. Springer, Berlin, 1993.

38. Xiaoli, M., Lin, Y. S., Wei, X. & Kniep, J. Ultrathin Carbon Molecular Sieve Membrane for Propylene/Propane Separation. *AIChE J.* **62,** 491–499 (2016).

39. Pan, Y., Li, T., Lestari, G. & Lai, Z. Effective separation of propylene/propane binary mixtures by ZIF-8 membranes. *J. Memb. Sci.* **390–391,** 93–98 (2012).

40. Kwon, H. T., Jeong, H. K., Lee, A. S., An, H. S. & Lee, J. S. Heteroepitaxially Grown Zeolitic Imidazolate Framework Membranes with Unprecedented Propylene/Propane Separation Performances. *J. Am. Chem. Soc.* **137,** 12304–12311 (2015).

41. Okamoto, K., Noborio, K., Hao, J., Tanaka, K. & Kita, H. Permeation and separation properties of polyimide membranes to 1,3-butadiene and n-butane. *J. Memb. Sci.* **134,** 171–179 (1997).

42. Ito, A. & Hwang, S.-T. Permeation of propane and propylene through cellulosic polymer membranes. *J. Appl. Polym. Sci.* **38,** 483–490 (1989).

43. Huang, Y., Merkel, T. C. & Baker, R. W. Pressure ratio and its impact on membrane gas separation processes. *J. Memb. Sci.* **463,** 33–40 (2014).

Highlights

- An optimization model of the hybrid process has been developed and solved in GAMS.
- The hybrid process can potentially reduce OPEX by 50%.
- The membrane properties have been optimized implementing an upper-bound equation.